Study by electrical conductivity measurement of redox properties of vanadium antimonate and mixed vanadium and iron antimonate

J.M.M. Millet[a,*], I.C. Marcu[a], J.M. Herrmann[b]

[a] *Institut de Recherches sur la Catalyse, CNRS, associé à l'Université Claude-Bernard, Lyon I, 2 avenue A. Einstein, F-69626 Villeurbanne Cedex, France*
[b] *Laboratoire de Chimie appliquée à l'Environnement, UMR 5634 CNRS, Université Claude-Bernard Lyon I, 43 Bvd du 11 novembre 1918, F-69622 Villeurbanne Cedex, France*

Abstract

The redox properties of vanadium and mixed vanadium and iron have been studied by electrical conductivity measurements. The solids which are active catalysts in the ammoxidation of propane, were shown to be n-type semiconductors with electrons as the main charge carriers. The changes in the electrical conductivity during alternative exposures to propane, oxygen and mixtures of propane and oxygen have been studied at 753 K. The pure vanadium antimonate became a p-type semiconductor after reduction under propane whereas the pure iron antimonate remained an n-type semiconductor. An intermediate behavior was observed for the mixed vanadium and iron compound. The changes in type of electrical conductivity have been explained by a surface transformation with the formation of antimony oxide and a rutile-type solid solution with only cationic vacancies. Such a transformation was limited when iron substitutes vanadium and was absent in pure iron antimonate.

1. Introduction

Vanadium antimonates are known to be efficient catalyst for the ammoxidation of propane [1–3]. It is commonly admitted that the active phase of these catalysts is the $VSbO_4$ phase. Its structure is derived from TiO_2 rutile-type, with two Ti^{4+} cations formally substituted by one V and Sb cation with however a cation deficiency [4]. This cation deficiency has been shown to be related to the presence of V^{4+}, leading to the formula $V_{0.64}^{4+}V_{0.28}^{3+}Sb_{0.92}^{5+}\square_{0.16}O_4$ where $\square$ stands for cationic vacancy [5].

We have recently shown that iron could substitute to vanadium and that a continuous solid solution was formed in the $VSbO_4$–$FeSbO_4$ system [6]. At low loading, iron appeared to substitute V^{4+} with a resulting charge discrepancy balanced by oxygen vacancies. Simultaneously, cationic vacancies remained present in the solid with even a small increase of their content so that a maximum of both types of vacancies was observed between 10 and 20% of iron substitution. We have shown that such modification generated very active sites for propane activation but more selective to form propene than acrylonitrile. Iron loading higher than 60%, induced the disappearance of V^{4+} and cationic vacancies, as well as the substitution of V^{3+} by Fe^{3+} in the lattice structure. It decreased the activity but increased the selectivity to acrylonitrile.

In order to understand the catalytic properties of the vanadium antimonate and to specify the reasons of the changes in the catalytic properties observed with the substitution of vanadium by iron, we have characterized by electrical

* Corresponding author. Tel.: +33 472445317; fax: +33 472445399.
E-mail address: millet@catalyse.cnrs.fr (J.M.M. Millet).

conductivity measurements, the redox properties of pure vanadium and iron antimonates and of a mixed vanadium–iron antimonate. The vanadium–iron antimonate was chosen with a stoichiometry corresponding to 10% of vanadium substitution, in the range that led to the highest increase in catalytic activity.

2. Experimental

Pure vanadium antimonate $VSbO_4$ (VSb) and vanadium antimonate partially substituted by iron $Fe_{0.10}V_{0.90}SbO_4$ (10FeVSb) were prepared by adding Sb_2O_3 to a NH_4VO_3 (and a $Fe(NO_3)_3·9H_2O$) solution; the resulting mixture was heated under reflux and stirred for 18 h and evaporated. The resulting solid powder was subsequently dried at 353 K before calcination at 623 and 973 K for 3 h, respectively. Pure iron antimonate $FeSbO_4$ (FeSb) has been prepared by heating $Fe(NO_3)_3·9H_2O$ to 353 K and adding Sb_2O_3 under stirring. The solution obtained was neutralized using NH_4OH, filtered and dried at 383 K for 24 h. The resulting solid was calcined at 773 K for 20 h and 1173 K for 2 h. $FeSbO_4$ has been prepared by heating $Fe(NO_3)_3·9H_2O$ to 353 K and adding under stirring Sb_2O_3 and NH_4VO_3. The solution obtained was neutralized using NH_4OH, filtered and dried at 383 K for 24 h. The resulting solid was calcined at 773 K for 20 h and at 1173 K for 2 h. Crystal structures of the samples were controlled by X-ray diffraction using a Siemens D5005 diffractometer and Cu Kα radiation. The specific surface areas were measured by the BET method using nitrogen adsorption at 77 K. XPS measurements were performed before and after catalytic tests, with a VG ESCALAB 200 R. Charging of catalysts samples was corrected by setting the binding energy of adventitious carbon (C 1s) at 284.5 eV. The experimental accuracy on XPS quantitative measurements was considered to be around 10%.

The electrical conductivity measurements (EC) of the catalysts were carried out in a static cell as previously described [7]. The powdered sample (575 mg) was placed between two platinum circular electrodes under a constant mechanical pressure ca. 10^5 Pa. There results a sample thickness t of 0.4 cm. The temperature of both electrodes was given by two soldered thermocouples whose wires were also used, when short-circuited, as conductors for electrical measurements. The electrical resistance of the samples was measured, according to the range investigated, with a Kontron multimeter (model DMM 4021) or with a digital teraohmmeter (Guildline Instruments, model 9520). The samples behaved as bulk conductors and the apparent electrical conductivity σ (Ω^{-1} cm^{-1}) was expressed by the formula: $\sigma = (1/R)(t/S)$, where R is the electrical resistance, and t/S the geometrical factor including the thickness t and the cross-sectional area S of the electrodes (diameter 1.00 cm). The measurements have been carried out under programmed temperatures with a heating rate of 5 K min^{-1} or under different oxygen partial pressures. To obtain information on the solids under con-

ditions as close as possible to those of catalysis, the measurements have then been performed at reaction temperature (753 K) during sequential periods under pure propane (165 Torr) and oxygen (65 Torr) and under propane–oxygen reaction mixtures corresponding approximately to the catalytic test ratio (165 Torr:65 Torr) (1 Torr = 133.3 Pa). Prior to the different gas admissions the cell was evacuated (10^{-3} Torr).

Indeed these measurements are only two probe measurements. However, it has previously been calculated that the number of exposed Pt_s atoms of both electrodes was small and negligible with respect to the total number of active sites of solid introduced in the cell. Furthermore, the problem of the electrode solid-interface had previously been examined and effects induced by the electrodes have never been observed [7]. The electrical field used was chosen at its minimum value compatible with the R measurements, i.e. 1 V. In addition, no differences in R measurements were observed in dc and ac current, indicating the absence of interface effects such as polarization.

3. Results and discussion

3.1. Physico-chemical characterization of the fresh and used catalysts

The results of the characterization of the prepared solids have been presented earlier [6]. The crystal rutile structures of the samples were checked by X-ray diffraction before and after catalytic tests and the chemical compositions of the samples were determined by atomic absorption. The results of these analyses along with those of other characterization techniques such as xanes, infra-red and Mössbauer spectrsocopies allowed the determination of the respective stoichiometries of the compounds which were: $V_{0.64}{}^{4+}V_{0.28}{}^{3+}Sb_{0.92}{}^{5+}\square_{0.16}O_4$, $Fe_{0.09}{}^{3+}V_{0.52}{}^{4+}V_{0.32}{}^{3+}Sb_{0.92}{}^{5+}\square_{0.18}O_{3.95}$ and $FeSbO_4$ [6].

XPS technique was used to characterize the catalysts before and after catalytic test (Table 1). The antimony surface content was systematically higher than that previously determined by chemical analysis whereas that of the iron was lower [6]. During the catalytic tests, the surface composition changed following two types of variation. The first one

Table 1

Atomic surface composition of the solids calculated from XPS, before and after catalytic test and after electrical conductivity measurement (e.c.m.)

Catalysts	Surface composition				
	Fe/(Fe + V)		Sb/(V + Fe)		After e.c.m.
	Before test	After test	Before test	After test	
VSb	0.00	0.00	1.3	2.5	1.6 (1.0)
10FeVSb	0.04	0.08 (0.10)	1.1	1.4	(1.0)
FeSb	1.00	1.00	1.3	1.1	(1.0)

The corresponding atomic bulk compositions, calculated from chemical analyses in Ref. [6], are given into parentheses.

corresponded to the increase of the iron surface composition for iron-containing compounds, tending closely to the bulk value. The second variation indicated the increase of the surface antimony composition of the vanadium-containing compounds. This last increase was much higher for VSb than for 10FeSb. The same effect of iron on the stabilization of the surface composition has also been observed for the other mixed vanadium and iron compounds with higher iron content [6]. The vanadium antimonate has been characterized after electrical conductivity measurement and showed an increase of the antimony surface composition as after catalytic test, but in a lower extent (Table 1).

3.2. EC measurements: Influence of temperature and oxygen partial pressure

The electrical conductivity of the compounds was measured from 295 to 775 K. The different curves obtained showed a regular increase of the conductivity with temperature except at low temperature (373 K) where a small peak was observed (Fig. 1). This variation has been attributed to surface dehydration with the suppression of surface conductivity by protons, which can move from one adsorbed water molecule to one another. Fig. 2 shows the variations of $\log \sigma$ versus reciprocal temperature under oxygen at atmospheric pressure between 373 and 753 K. The linear variations observed showed that all the compounds behaved as semiconductors whose electrical conductivities varied exponentially with temperature according to the typical activation law:

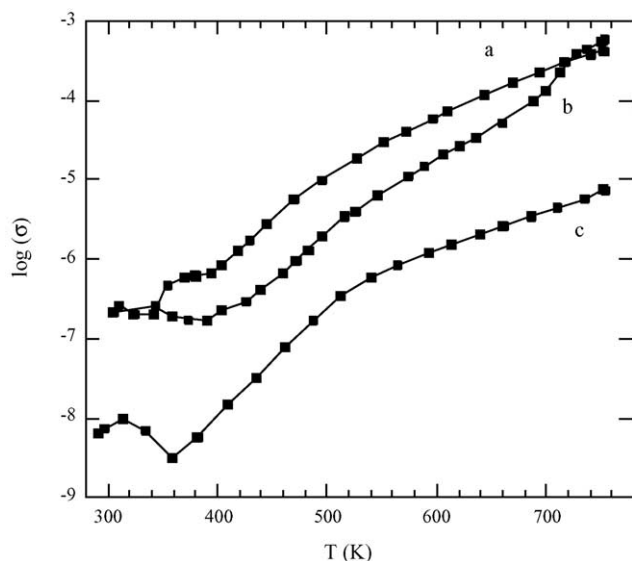$$\sigma = \sigma_0 \exp\left(-\frac{E_c}{RT}\right) \tag{1}$$

Fig. 1. Semilog plot of σ variation as a function of the temperature during temperature-programmed heating of the antimonate catalysts, VSb (a), 10FeVSb (b) and FeSb (c), under dynamic vacuum from 295 to 755 K (heating rate 5 °C min^{-1}); σ in Ω^{-1} cm^{-1}.
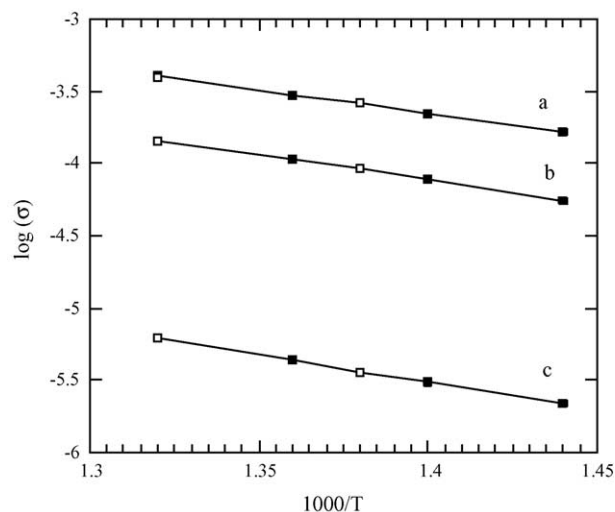

Fig. 2. Arrhenius-type semilog plot $\log \sigma = f(1/1000T)$ of curves of Fig. 1: VSb (a), 10FeVSb (b) and FeSb (c) (($\blacksquare$) under increasing oxygen pressure, ($\square$) under decreasing oxygen pressure).

where σ_0 is the preexponential factor and E_c is the dynamic activation energy of conduction. The dynamic activation energies of conduction (E_c) have been calculated for the different solids and found to be quite similar (Table 2). The evolution isotherms of the electrical conductivity as a function of the oxygen partial pressure were studied at 753 K. Fig. 3 shows the variations of σ as a function of P_{O_2} in a log–log plot. It clearly appeared that all the solids were of the n-type under oxygen since $\partial \sigma / \partial P_{O_2} < 0$. For FeSbO$_4$ this result confirmed that previously obtained by Tianshu and Hing, who had already determined its semi-conduction type [8].

It is generally assumed that the electrical conductivity σ of oxides varies as a function of residual partial pressure P_{O_2} and temperature T, according to the equation:

$$\sigma(P_{O_2}, T) = C P_{O_2}^{1/n} \exp\left(-\frac{\Delta H_c}{RT}\right) \tag{2}$$

where ΔH_c represents the enthalpy of conduction and C is a constant which only depends on various characteristics of the powdered sample (charge and mobility of the charge carriers, number of contact points between grains, etc.) [7]. When the exponent n is equal to an integer; its value can be indicative of the nature of the solid defects, which generate charge carriers. Its algebraic sign indicates the type of semi-conduction (n or p).

Table 2
E_c activation energy of conduction and n exponent of Eq. (2) for the different solids

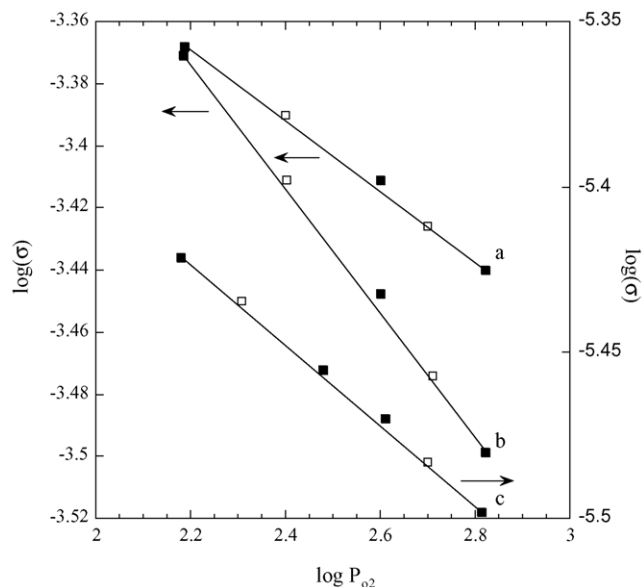| Catalysts	E_c (kJ mol^{-1})	n
VSb	61.0	9.5
10FeVSb	65.1	8.0
FeSb	72.6	4.5

Fig. 3. Plots of log $\sigma = f(\log P_{O_2})$ for VSb (a), 10FeVSb (b) and FeSb (c) at 753 K (($\blacksquare$) under increasing oxygen pressure, ($\square$) under decreasing oxygen pressure).

The values of exponent n calculated for the different solids are presented in Table 2. From these values, only FeSb behaved according to a simple conduction model with n approximately equal to -4. Such a value corresponds to the formation of singly ionized anionic vacancies according to the equations:

$$O^{2-} \leftrightarrows \tfrac{1}{2}O_2(g) + V_O \qquad (3)$$

$$V_O \leftrightarrows V_O{}^\bullet + e^- \qquad (4)$$

with $K_{[3]} = P_{O_2}^{1/2}[V_O]$ and $K_{[4]} = [V_O{}^\bullet][e^-]/[V_O]$ V_O and $V_O{}^\bullet$ represent anionic vacancies with respectively two and one electrons trapped. The electroneutrality condition ($[e^-] = [V_O{}^\bullet]$) combined with the mass action law yields:

$$[e^-] = [(K_{[3]})_0(K_{[4]})_0]^{1/2} \exp\left[-\frac{\Delta H_{[3]} + \Delta H_{[4]}}{2RT}\right] P_{O_2}^{-1/4} \qquad (5)$$

where $\Delta H_{[3]}$ and $\Delta H_{[4]}$ are the enthalpies of reactions (3) and (4). Generally, the ionization energy of the first electron $\Delta H_{[4]}$ can be neglected with respect to the formation enthalpy of anionic vacancies $\Delta H_{[3]}$. Consequently, the heat of formation of anionic vacancies is equal to $2E_c$, corresponding for FeSb to 145.2 kJ mol^{-1} per mole of vacancies. This enthalpy could appear substantially smaller than that observed for other n-type pure oxides such as titania (342.7 kJ mol^{-1}) [9] or tin oxide (226 kJ mol^{-1}) [10]. However, this low value could be responsible for a higher lability of surface lattice anions able to react with the mixture (propene + ammonia) in the ammoxidation of C_3H_6 into acrylonitrile. Under our experimental conditions, FeSbO$_4$ was efficient, as an n-type

semiconductor, for propene ammoxidation but not for that of propane [6]. The case study of the two vanadium containing antimonates was more complex. The n values calculated for these compounds, 8 and 9.5, were significantly higher than 4 or 6 that respectively correspond to the formation of singly and doubly ionized vacancies. Such phenomenon could be explained by a more complex model involving two different sources of electrons, one being independent of the partial pressure of oxygen while the other one is related to defects connected to it such as anionic vacancies:

$$\sigma = \sigma_1 + \sigma_2 \qquad (6)$$

with $\sigma_1 = A(K_{[3]}K_{[4]})^{1/2} P_{O_2}^{-1/4}$ and σ_2 independent of P_{O_2}. Such a model, which does not correspond to a mixture of oxides but just to a mixed conduction process, has already been proposed for TiO$_2$ and related compounds [11]. In the present study, a linear relationship was obtained when plotting σ as a function of $P_{O_2}^{-1/4}$ (Fig. 4). This confirmed the existence of a source of conduction electron whose nature was independent of oxygen pressure.

3.3. EC measurements under subsequent gaseous atmospheres: propane, oxygen and propane–oxygen mixture

The results of this study are presented in Fig. 5. To study the influence of propane and of oxygen on the electrical conductivity, the catalysts were heated in air and, after a rapid evacuation of the cell, propane was introduced. Immediately the electrical conductivity of the three solids increased abruptly. Propane reduced the catalyst, which behaved as a typical n-type semiconductor. After reaching steady state un-
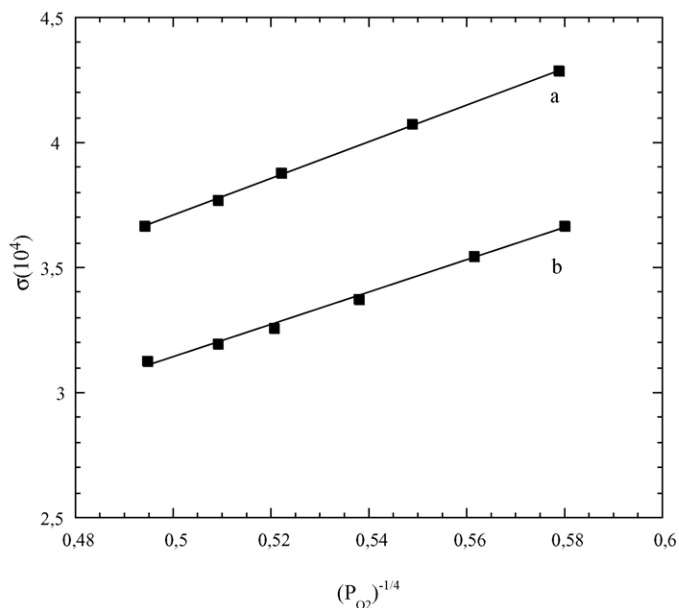

Fig. 4. Linear transforms of $\sigma = f(P_{O_2}^{-1/4})$ for the VSb (a) and 10FeVSb (b) compounds at 753 K.
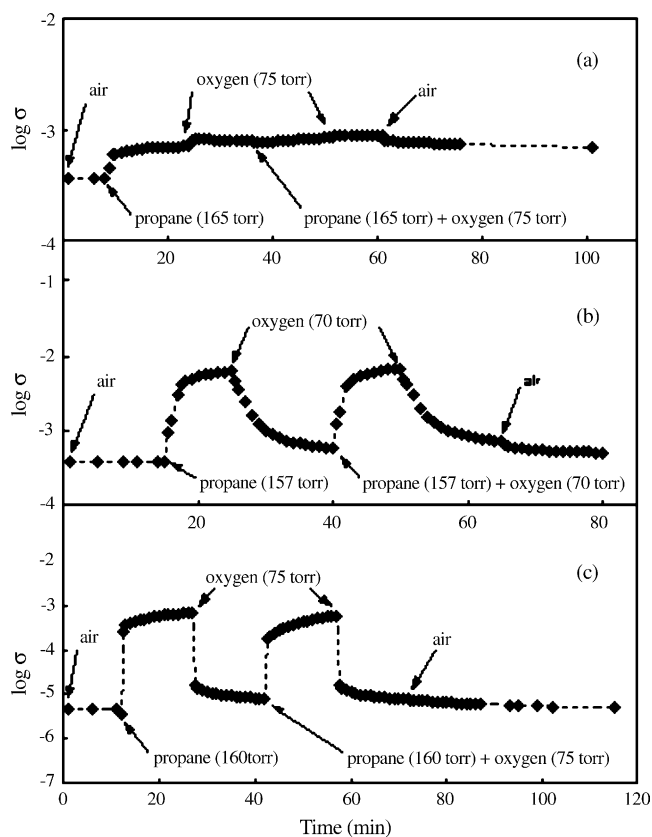
Fig. 5. Variations of the logarithm of the electrical conductivity at 753 K under sequential exposures to air, propane, oxygen and propane–oxygen reaction mixture for VSb (a), 10FeVSb (b) and FeSb (c).

der propane, the cell was again evacuated and replaced by pure oxygen. For 10FeVSb and FeSb compounds, the electrical conductivity decreased as anticipated for n-type semiconductors. By contrast, for VSb, the electrical conductivity slightly increased. This appeared more clearly when σ was directly plotted as a function of the sequence duration (Fig. 6). Such phenomena were reproducible and appeared also under the propane–oxygen sequences.

The results obtained on VSb showed that it was an n-type semiconductor but that after reduction it behaved as a p-type semiconductor. Such a phenomenon can only be explained
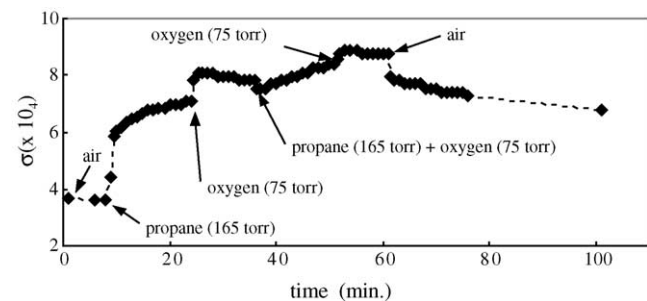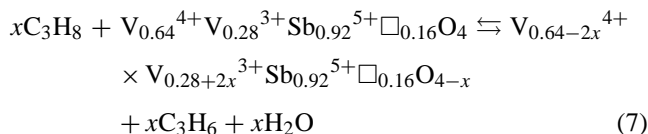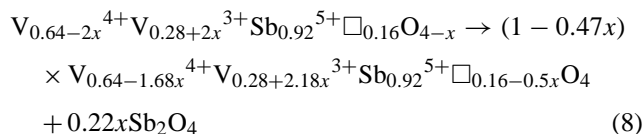

Fig. 6. Variation of the electrical conductivity σ at 753 K under sequential exposures to propane, oxygen and propane–oxygen mixture for VSb.

by a change in the structure of the compound, at least in the surface region. The existence of such irreversible change was supported by the fact that after the first reduction, the solid underwent redox cycles that were not reversible and remained characteristic of a p-type semiconductor. Because this change should be limited to the surface of the solid, it was not observed by X-ray powder diffraction. However, XPS analyses indicated that the surface composition changed during the electrical conductivity measurement as well as during the catalytic test with an apparent surface enrichment in antimony oxide.

It can be assumed that the increase of electrical conductivity under propane was related to that of the free electron concentration originating from the creation of ionized anionic vacancies. Propane reduced the oxygen surface lattice of the phase and created anionic vacancies according to the reaction:

$$
\begin{aligned}
x\mathrm{C_3H_8} + \mathrm{V_{0.64}}^{4+}&\mathrm{V_{0.28}}^{3+}\mathrm{Sb_{0.92}}^{5+}\square_{0.16}\mathrm{O_4} \leftrightarrows \mathrm{V_{0.64-2x}}^{4+} \\
&\times \mathrm{V_{0.28+2x}}^{3+}\mathrm{Sb_{0.92}}^{5+}\square_{0.16}\mathrm{O_{4-x}} \\
&+ x\mathrm{C_3H_6} + x\mathrm{H_2O}
\end{aligned} \tag{7}
$$

The solid formed containing both cationic and anionic vacancies should not be stable and a phase transformation should occur leading to a vanadium antimonate: (i) richer in vanadium and (ii) supporting an antimony oxide partially coating the surface:

$$
\begin{aligned}
\mathrm{V_{0.64-2x}}^{4+}&\mathrm{V_{0.28+2x}}^{3+}\mathrm{Sb_{0.92}}^{5+}\square_{0.16}\mathrm{O_{4-x}} \rightarrow (1-0.47x) \\
&\times \mathrm{V_{0.64-1.68x}}^{4+}\mathrm{V_{0.28+2.18x}}^{3+}\mathrm{Sb_{0.92}}^{5+}\square_{0.16-0.5x}\mathrm{O_4} \\
&+ 0.22x\mathrm{Sb_2O_4}
\end{aligned} \tag{8}
$$

This interpretation can be supported by the fact such a composition can be obtained when the vanadium antimonate was prepared with a heat treatment under nitrogen [12]. Such a behavior of vanadium antimonate means that, it contained after reduction only cationic vacancies and mainly vanadium with its lower oxidation state ($\mathrm{V^{3+}}$), typical of a p-type semiconductor such as NiO [13]. It could be noted that the same segregation was already observed in SnSbO system [14]. We have recently shown that at a low substitution level ($x < 0.4$ in $\mathrm{Fe_xV_{1-x}SbO_4}$), $\mathrm{Fe^{3+}}$ substituted to $\mathrm{V^{4+}}$ in the cationic deficient structure of vanadium antimonate leading to a structure with both cationic and anionic vacancies. For the 10FeVSb, the calculated stoichiometry corresponded to: $\mathrm{Fe_{0.09}}^{3+}\mathrm{V_{0.32}}^{3+}\mathrm{V_{0.52}}^{4+}\square_{0.18}\mathrm{Sb_{0.94}}^{5+}\mathrm{O_{3.95}}$. The substitution of vanadium by iron allowed the stabilization of the reduced compound with a structure presenting both cationic and anionic vacancies without phase transformation [6]. Such stabilization effect induced by iron had previously been observed in Fe–Sn–Sb–O system [15]. The solid then always behaved as an n-type semiconductor under oxygen and during the following redox cycle under catalytic propane–oxygen mixtures. The fact that the electrical conductivity cycles

were not exactly reversible could account for a slight transformation of the surface as shown by XPS measurements. Both types of semiconductivity may co-exist and account for the behavior of the 10FeVSb catalyst. For FeSb the results obtained were typical of a pure n-type semiconductor behavior.

3.4. Consequences for catalysis

Because of the p-type character of the VSb catalyst, the same activation mechanism of propane as that first postulated by Aika and Lundsford some years ago, has been proposed [16]. It is based upon the formation of hydrocarbon radicals initiated by positive holes p^+ holes, related to the presence of cationic vacancies [6]. These positive holes correspond to electron vacancies in the valence band of O^{2-} that can be filled by electrons hopping from neighbouring anion leading to the equivalent equation:

$$O^{2-} + p^+ \leftrightarrows O^- \tag{9}$$
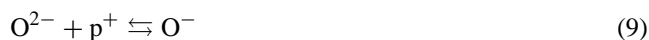
Propane activation could proceeds with a C−H bond cleavage via the attack by a hole:

$$C_3H_8 + p^+ \leftrightarrows C_3H_7^\bullet + H^+ \tag{10}$$

The chemical support of a hole p^+ being an O^- species, Eq. (10) can also be written as

$$C_3H_8 + O^- \leftrightarrows C_3H_7^\bullet + O^{2-} + H^+ \tag{11}$$
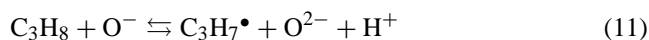
The radical formed would undergo a second hydrogen abstraction according to a similar mechanism leading to propene. It could be outlined that such a process is similar to that encountered in the oxidation of *n*-butane on $(VO)_2P_2O_7$ [17] or on TiP_2O_7 [18,19] which are p-type semiconductors.

In 10FeVSb, the presence of Fe^{3+} allowed the stabilization of the compound with more anionic vacancies in reducing conditions and limit the formation of surface antimony oxide as shown from electrical conductivity measurements with mostly a n-type semiconductor behavior under propane. In this case the activation of propane would be related to the presence of isolated V species, which have been proposed to be the most active species [20] and that should correspond to the V^{4+}–O^- already suggested as activation site by Grasselli [21] and Andersson et al. [22]. It is difficult to know if the concomitant presence of anionic vacancies may play a role or not. The increase in selectivity to propene detrimental to that in acrylonitrile or CO_2 may be explained by the absence of antimony oxide at the surface of the active phase, which has been shown to be responsible for the selective synthesis of acrylonitrile from intermediate propene [23], or by the presence of the anionic vacancies that limits the number of active oxygen species available for the further transformation of the propene or intermediate formed. The presence of these anionic vacancies in catalytic conditions was clearly demon-

strated by the electrical conductivity measurements data and the n-type semiconductivity observed.

4. Conclusions

The present study established the n-type semiconductor character of $VSbO_4$, which is considered as the active phase in the selective ammoxidation of propane. However, it has been observed that $VSbO_4$ behaved as a p-type semiconductor under propane or under oxygen–propane mixture. This could be explained by a surface transformation with the formation of antimony oxide and a rutile phase richer in vanadium. Such transformation could account for the surface antimony enrichment observed by XPS.

$VSbO_4$ with vanadium partially substituted by iron, as well as $FeSbO_4$, appeared also as n-type semiconductors. They kept the same type of conductivity under propane or propane–oxygen mixture. In the case of the mixed vanadium and iron antimonate, the absence of a total reversibility of the electrical conductivity supported a partial modification of the surface with a small increase in antimony surface content.

Because $VSbO_4$ transforms under catalytic reaction conditions with the appearance of a p-type character, the activation mechanism of propane on $VSbO_4$ could be based upon the formation of hydrocarbon radicals on O^-, which are oxidizing species strong enough to attack alkanes C−H bonds. Although that when Fe substituted partially V, the n-type of semiconductivity was kept, the same type of activation could be carried but it would be related to the presence of isolated V species.

References

[1] J.R. Ebner, US Patent 4,405,498 (1983).
[2] A.T. Guttmann, R.K. Grasselli, J.F. Brazdil, US Patent 4,746,641, 4,788,317 (1988).
[3] R. Nilsson, T. Lindblad, A. Andersson, J. Catal. 148 (1994) 501.
[4] T. Birchall, A.E. Sleight, Inorg. Chem. 15 (1976) 868.
[5] S. Hansen, K. Stahl, R. Nilsson, A. Andersson, J. Solid State Chem. 102 (1993) 340.
[6] H. Roussel, B. Mehlomakulu, F. Belhadj, E. van Steen, J.M.M. Millet, J. Catal. 205 (2002) 97.
[7] J.M. Herrmann, in: B. Imelik, J.C. Védrine (Eds.), Catalyst Characterization, Physical Techniques for Solid Materials, Plenum Press, New York, 1994, p. 559 (Chapter 20).
[8] Z. Tianshu, P. Hing, J. Mater. Sci.: Mater. Electron. 10 (1999) 509.
[9] J.M. Herrmann, J. Catal. 118 (1989) 43.
[10] J.M. Herrmann, J.L. Portefaix, M. Forissier, F. Figueras, P. Pichat, J. Chem. Soc., Faraday Trans. 1 (75) (1979) 1346.
[11] J.M. Herrmann, J. Disdier, Catal. Today 20 (1994) 135.
[12] F.J. Berry, M.E. Brett, J. Chem. Soc., Dalton Trans. (1983) 9.
[13] C.M. Osburn, R.W. West, J. Chem. Solids 32 (1971) 1331.
[14] J.M. Herrmann, J.L. Portefaix, React. Kinet. Catal. Lett. 12 (1979) 51.
[15] B. Benaïchouba, J.M. Herrmann, React. Kinet. Catal. Lett. 22 (1983) 209.
[16] K. Aika, H. Lundsford, J. Phys. Chem. 81 (1977) 1393.

[17] J.M. Herrmann, P. Vernoux, K. Béré, M. Abon, J. Catal. 167 (1997) 106.

[18] I.C. Marcu, J.M.M. Millet, J.M. Herrmann, Catal. Lett. 78 (1–4) (2002) 273.

[19] I.C. Marcu, I. Sandulescu, J.M.M. Millet, Appl. Catal. A 227 (1–2) (2002) 309.

[20] D.L. Nguyen, Y. Ben Taarit, J.M.M. Millet, Catal. Lett. 90 (1–2) (2003) 65.

[21] R.K. Grasselli, in: G. Ertl, H. Knözinger, J. Weitkamp (Eds.), Handbook of Heterogeneous Catalysis, vol. 5, Wiley–VCH, 1997, p. 2307.

[22] A. Andersson, S.L.T. Andersson, G. Centi, R.K. Grasselli, M. Sanati, F. Trifiro, in: L. Guczi, F. Solymosi, P. Tetenyi (Eds.), Stud. Surf. Sci. Catal. 7 (1992) 691.

[23] G. Centi, S. Perathoner, in: G. Poncelet, et al. (Eds.), Stud. Surf. Sci. Catal. 92 (1995) 59.